Starch - Stärke

WILEY-VCH
Starch

RESEARCH ARTICLE

Sago Starch Reinforced With Cellulose Microfibers Isolated From *Dialium cochinchinense* Residue

Polphat Ruamcharoen[1,2] | Purintorn Chanlert[2] | Chumphon Numuang[3] | Lapporn Vayachuta[4] | Jareerat Ruamcharoen[3]

[1]Rubber and Polymer Technology Program, Faculty of Science and Technology, Songkhla Rajabhat University, Muang, Songkhla 90000, Thailand | [2]Research Unit in Applied Physics and Advanced Materials, Faculty of Science and Technology, Songkhla Rajabhat University, Muang, Songkhla 90000, Thailand | [3]Faculty of Science and Technology, Prince of Songkla University, Muang, Pattani 94000, Thailand | [4]National Nanotechnology Center (NANOTEC), National Science and Technology Development Agency (NSTDA), Khlong Luang, Pathum Thani 12120, Thailand

Correspondence: Jareerat Ruamcharoen (jareerat.su@psu.ac.th)

Received: 29 January 2025 | **Revised:** 17 February 2026 | **Accepted:** 3 March 2026

Keywords: biocomposites | cellulose microfiber | sago starch | velvet tamarind peel | water resistance

ABSTRACT

This research investigated the development of sago starch (SS) film reinforced with velvet tamarind (*Dialium cochinchinense*) peels for potential biopolymer film applications. SS was gelled at 80°C and plasticized with glycerol. After that, VT and treated VT (TVT) fibers were incorporated with content of 1, 3, and 5 wt%. The SS, SS_VT, and SS_TVT biocomposites were systematically evaluated for their transparency, water resistance and tensile properties. The addition of VT and TVT significantly improved ultraviolet (UV) protection, although this improvement was accompanied by a decrease in visible light transparency. Water absorption and water vapor transmission of the biocomposite films also decreased compared to neat SS. Moreover, the biocomposite films exhibited substantially higher tensile strength (TS) and Young's modulus (YM) than neat SS film. Notably, the composite film containing 3 wt% VT demonstrated the highest TS and YM value. This confirmed the effective dispersion of 3 wt% of VT within starch matrix and strong interface interaction between cellulose fibers and starch, as revealed by FTIR and SEM analysis. The thermal degradation temperatures of biocomposite films containing 1 wt% VT and TVT were shifted to higher values compared to that of the starch matrix. The incorporation of VT and TVT enhanced the tensile properties of the biocomposite films; however, TVT-reinforced films showed relatively inferior performance compared to VT reinforced films, primarily due to increased particle agglomeration, as observed by SEM. Totally, SS films reinforced with VT show strong potential for biopolymer packaging applications, owing to their improved water resistance and mechanical properties.

1 | Introduction

Green and circular economy principles are reshaping industrial approaches across various industries. Inspired by bioeconomy ideas, the replacement of conventional materials derived from natural resources with waste by-products from agriculture and industry are currently investigation [1, 2]. As consumers prioritize sustainability and demand eco-friendly packaging, alongside growing product complexity and heightened environmental awareness, there is a strong emphasis on supporting a circular economy and reducing carbon emissions. In recent decades, there has been significant progress in reducing the carbon footprint of industrial products and innovations in packaging, such as biodegradable and smart packaging [3, 4]. The trend toward renewable and biodegradable materials is gaining momentum, driven by increasing environmental awareness among the general population, corporations, and governments. Therefore, developing polymers enhanced with natural polymers and fibers are

an intriguing alternative [4–7]. These materials provide benefits such as partial or full renewability, biodegradability, lower energy consumption in production, and adequate mechanical properties for a wide range of applications [6, 7]. One of the most important uses of biodegradable polymers reinforced with natural fillers is in the realm of food packaging, a focus shared by numerous researchers [7–9]. Presently, starch is gaining attention from the bioplastics industry. Because starch is an agricultural raw material that can be grown as a replacement, it is cheap and easily available from a variety of crops such as cassava, corn, sago palm, and so fourth [10–12].

Sago palm is a valuable resource, especially in rural areas, because of its wide range of uses, especially in the production of flour, whether it be sago flour. The development of biodegradable packaging materials has a great deal of promise for exploration. However, the mechanical properties, gas and moisture (MS) barriers of packaging films made from starch are insufficient because of their high hydrophilic content. Their potential as an essential raw material to produce biodegradable packaging materials is so constrained. As a result, many studies have been conducted to improve the properties of starch through incorporating plasticizers and fillers [12–14].

Natural fibers exhibit desirable characteristics such as high specific strength, low density, recyclability, cost-effectiveness, and a high modulus. Notably, they can be utilized as bio-fillers, offering significant potential to reinforce and enhance the mechanical performance of polymers [15–17]. Cellulose fiber is among the most important representatives of natural fibers, recognized for its abundance and desirable mechanical properties. As a polysaccharide, it can be extracted from a variety of plants or agricultural wastes, such as rice husk, walnut shell, oil palm fiber, pineapple and banana leaf fiber, coffee grounds, and so forth [15, 18–22]. Since these plant fibers are mainly chemically composed of cellulose, hemicellulose and lignin having a strong molecular structure which can be used as reinforcing materials. These fillers are crucial to the structure, serving as reinforcing agents that enhance the mechanical properties by transferring the tension from the matrix to the filler, and improving the water-barrier properties of the composites through the tortuous pathway and the inter- and intra-interactions between the filler and the matrix [21–24]. Previous reports have shown that the addition of apricot and walnut shell powders can improve the tensile properties (modulus and tensile strength [TS]) of starch-based films [20]. Cellulose microfiber was extracted from the *Musa saba'* banana midrib residue using several chemical treatments, including steam explosion, alkaline treatment, acid-chlorite treatment, and acid hydrolysis. Incorporating 1 wt% of microfibers into a starch-based biofilm increased mechanical properties, opacity, and crystalline while elongation at break (EB) decreased as compared to biofilm without cellulose microfibers [17, 22].

The velvet tamarind (VT) is a large evergreen tree, scientifically known as *Dialium cochinchinense*, found in southern Thailand. Its production generates significant annual income for farmers. However, VT peels are a waste material generated by community enterprise processing, which creates management problems and environmental impacts. VT fruits are clustered, with black skin, orange flesh, and a friable texture. The VT peel is expected to be a potential filler, which has not been previously reported. The utilization of natural fibers-reinforced composites has been steadily increasing; however, the market remains relatively specialized, primarily due to challenges such as achieving strong interfacial adhesion between the fibers and the matrices. Starch-based composites are expected to offer several notable advantages, including superior TS derived from the inherent chemical compatibility between cellulose and starch, high water resistance resulting from the hydrophobic nature of the fibers, and complete degradability coupled with long-term sustainability [16, 24].

Given these considerations, the objective of this study was to incorporate cellulose extracted from VT (*D. cochinchinense*) peel as a reinforcing filler within a starch matrix. The effects of VT fiber type (FT) and filler loading on the physical and mechanical properties of starch-based composite films were systematically investigated. Target performance parameters, including water resistance, mechanical strength, and thermal behavior, were evaluated to assess the suitability of the composites for functional applications. Furthermore, the interfacial interactions between the starch matrix and VT or treated VT (TVT) fibers were examined using Fourier transform infrared spectroscopy (FTIR), x-ray diffraction (XRD), and scanning electron microscopy (SEM). These analyses were expected to elucidate the structure–property relationships governing the observed physical, mechanical, and thermal performance of the composite materials.

2 | Material and Methods

2.1 | Materials

Sago starch (SS) is the natural starch isolated from sago palms (*Metroxylon sagu* Rottb.) in Pattani, Thailand. VT rind (*D. cochinchinense*) was obtained from Dong Look Yee Community Enterprise Group, Pattani, Thailand. Glycerol used as a plasticizer was a product of Ajax Fine Chem. Pty Ltd. (Australia).

2.2 | Cellulose Microfiber Isolation and Treatment From VT Peel

2.2.1 | VT Fiber Isolation

The VT peel was first cleaned to remove surface dirt and impurities, followed by washing with distilled water and drying in an oven at 60°C for 24 h. The dried VT peel was finely ground by using a commercial herb grinder (WF-10B, Taiwan) and subsequently dried in a hot air oven. As a result, VT fiber retained their natural surface characteristics, including a high content of hydroxyl (–OH) groups from cellulose, hemicellulose, and residual lignin.

2.2.2 | Treatment of VT Fiber

The treatment of VT fiber was prepared according to Chanthavong et al. (2020) with some modification method [25]. The VT fiber was treated with 6 wt% NaOH solution, heated at 80°C for 2 h, followed by filtration and washing with distilled water until neutrality was achieved. The alkali-TVT was subsequently bleached with a 10 wt% H_2O_2 solution to obtain TVT microfibers,

which was then dried in an oven for 24 h. The chemical composition of the VT and TVT was determined, with lignin content of 34.2% and 18.4%, and cellulose content of 85.2% and 93.9%, respectively.

2.3 | Preparation of Biocomposite Films

Starch-based composite films were prepared using the solution-casting method, following the procedure described by Katong et al. [26]. SS was dispersed in distilled water and continuously stirred at 80°C for 15 min. The glycerol (30 wt% of starch) as a plasticizer was then added to starch solution and mixed with VT and TVT particles in varying amounts of 1, 3, and 5 wt% of starch. The resulting mixture was homogenized and poured into a polyethylene casting mold. The biocomposite films were dried in an oven at 50°C for 48 h. After drying, the starch-based composite film was removed from the casting plate and stored in a MS-controlled cabinet for further characterization.

2.4 | Biocomposite Film Characterization

2.4.1 | Morphology

The microstructure of VT, TVT, and biocomposite films was examined using a scanning electron microscope (Hitachi SU3500, Japan) operated at an accelerating voltage of 10 kV. Composite films were cryo-fractured in liquid nitrogen to reveal cross-section morphology. Subsequently, the samples were sputter-coated with a thin gold layer and observed at magnifications of 500X and 1000X.

2.4.2 | UV–Visible Transmission of Biocomposite Films

The UV–visible transmission of the biocomposite films was evaluated following the method described by Wahab et al. (2023) [22]. Rectangular film specimens (1×2 cm^2) were analyzed over a wavelength range of 200–800 nm using a Lambda 35 UV–visible spectrophotometer (PerkinElmer, United States). For each specimen, the light absorption values were recorded in triplicate.

2.4.3 | Moisture (MS) Content Test

The standard method for determining MS content in starch films involves drying the film and measuring the resulting weight loss, following ASTM D644-99. Starch-based composite films were cut into 2 cm × 2 cm specimens and weighed to obtain the initial weight (W_i). The specimens were then dried at 105 °C for 2 h until a constant weight (W_f) was reached. The MS content was calculated according to Equation (1).

$$\text{MS content}\,(\%) = \frac{W_i - W_f}{W_i} \times 100 \tag{1}$$

2.4.4 | Water Absorption (WA) Test

Specimens measuring 2 cm × 2 cm were weighed and dried in an air-circulating oven at 105 ± 2°C for 24 h to eliminate any MS. All samples were immersed in water at room temperature (25 ± 2°C) for 24 h, after that weighed again. The percentage of WA content was calculated using the following Equation (2).

$$\text{WA content}\,(\%) = \frac{W_{abs} - W_o}{W_o} \times 100 \tag{2}$$

where W_o is weight prior to absorption test, and W_{abs} is WA sample weight after testing, respectively. These measurements were performed in five replicates.

2.4.5 | Water Solubility (WS) Test

WS was measured as the percentage of dry film material that dissolved after 24 h of soaking in distilled water. The film specimens (2 cm × 2 cm) were weighed before the test (W_i) and then immersed in distilled water at room temperature for 3 months. After this period, the undissolved and dissolved portions were separated through filtration. The undissolved portion was then dried at 110°C for 6 h and weighed to record the results. The weight change of WS test was calculated following Equation (3).

$$\text{WS content}\,(\%) = \frac{W_i - W_{us}}{W_i} \times 100 \tag{3}$$

where W_i is sample weight before WS test, and W_{us} is weight of undissolved samples.

2.4.6 | Water Vapor Transmission (WVT) Test

The water vapor transmission rate (WVTR) was determined following the ASTM DE9600 method, as described by Ruamcharoen et al. [12]. Glass bottles were filled with 10 g of silica gel, and biocomposite films were cut into circular specimens with a diameter of 3.6 cm. Each film was placed over the mouth of a bottle and weighed to obtain the initial weight. The bottles were then placed in a desiccator maintained at 75% relative humidity (RH). The sample films were weighed at 6 h intervals until a constant weight was reached. The WVTR was calculated according to Equation (4).

$$\text{WVTR} = \frac{\Delta m}{t \times A} \tag{4}$$

where Δm is the weight change gained WVT (g), A is the WVT area (cm^2), and t is the interval time for WVT (h).

2.4.7 | Tensile Property Measurement

The tensile properties of the biopolymer films were evaluated using a Narin Universal Testing Machine (NRI-TS500-30B) equipped with a 1 kN load cell at a temperature of 25 ± 2°C and RH of 50% ± 5% according to ASTM D882 method. Five biocomposite films were cut into specimens measuring 10 cm × 1.2 cm. Each specimen was clamped between grips with an initial gauge length of 30 mm, and tests were performed at a crosshead speed of 50 mm.min^{-1}. The TS, elastic modulus, and percentage EB were recorded.

2.4.8 | Fourier Transform Infrared Spectroscopy

FTIR was employed to analyze the chemical structure and functional groups of VT, TVT, and biocomposite films. Measurements were conducted using a Bruker Tensor 27 spectrometer (United States), with samples exposed to infrared radiation over a wavenumber range of 400–4000 cm^{-1}, a resolution of 4 cm^{-1}, and a total of 16 scans.

2.4.9 | X-Ray Diffractometry

XRD analysis was conducted using an X'Pert Pro Diffractometer (Panalytical) in reflection mode with Cu-K_α radiation ($\lambda = 0.154$ nm). The samples were analyzed at 30 kV and 15 mA, covering a 2θ range of 5°–50°, with a scanning step of 0.02°/min and a step time of 10 s.

2.4.10 | Thermogravimetric Analysis (TGA)

Thermal stability of VT, TVT, and biocomposite film were investigated by using a Perkin Elmer TGA 8000 apparatus to assess weight changes within a temperature range of 50°C–600°C. This analysis was performed in a nitrogen gas atmosphere with a heating rate of 10°C/min.

2.4.11 | Statistical Analysis

All experiments were conducted in five replicates, and the results are presented as mean ± standard deviation (S.D.). Analysis of variance (ANOVA) using a quadratic model was performed to evaluate the significance of the independent variables and their interactions on the response variables (SAA and TLA). The analysis was performed using the "statsmodels" library in Python [27]. Two independent variables were considered: FT with two levels (VT and TVT) and fiber percentage (FP) with three levels (1, 3, and 5 wt%), respectively.

3 | Results and Discussion

3.1 | Appearance Characteristic of VT and TVT

Figure 1 illustrates the photograph and SEM images of VT and TVT subjected to the chemical treatment.

It can be observed that the inner surface of VT peel is flaky and brown while the outer surface is black and velvet-like as shown in Figure 1a. When the VT peel was ground into brown powder and sieved through a 100 μm sieve (Figure 1b), treated with alkaline solution and bleached, the TVT appeared to be yellow color. From SEM images (Figure 1d,e), it was found that VT has a smooth surface, irregular shape, and becomes rougher after alkaline treatment and bleaching processes. Because some impurities and noncellulosic materials were removed from VT as previously mentioned [28–30]. However, TVT particles were larger than that of raw VT. As considered by SEM images, it was found that TVT particles agglomerated into bundles resulting in the increment diameter of TVT particles. This observation indicates that the alkali treatment and H_2O_2 beaching could effectively remove some noncellulosic components and enhance the hydrogen bonding between cellulose chains [28, 30, 31].

3.2 | Visual Appearances and Light Transmittance of Biocomposite Films

Figure 2 displays the visual appearance and light transmittance of starch-based composite films. All biocomposite films were transparent, as the text on the paper was clearly visible. Upon observation, the neat starch film was completely transparent, whereas the biocomposite films became semi-transparent with the addition of VT and TVT. Increasing the VT and TVT content in the starch matrix, therefore, reduced the transparency of the biocomposite films.

The optical property of the composite film is of foremost importance when considering its use in food packaging. This property specifies the protection of food from exposure to light. Specifically, food deterioration is caused by ultraviolet (UV) radiation. Film transparency was investigated using the percentage of light transmittance [26, 32]. The VT particles addition reduced the transmittance in the UV regions (200–400 nm), compared with the neat starch film. Moreover, the transmission of biocomposite films also decreased with an increase in VT content as shown in Figure 2b. This effect can be attributed to the present microscale fibers, which exhibit low transparency and reflect more light, thereby enhancing the UV-shielding capacity of the starch-based films due to the reduced band gap energy [32, 33]. When comparing the biocomposites, films containing TVT were found to be more translucent than those containing VT. Increasing the VT and TVT content from 1 to 5 wt% significantly improved the shielding effectiveness for both UVB (280–315 nm) and UVA (315–400 nm) but also decreased visible light transparency. In comparison with SS_VT films, SS_TVT films exhibit lower transmittance primarily as a result of fiber surface treatment, which enhanced cellulose purity, crystallinity, dispersion and interfacial adhesion within the starch matrix. This can be advantageous for food packaging, especially for light-sensitive foods, as it helps prevent light-induced lipid oxidation [32].

3.3 | Water Resistance Characteristics

The water resistance of starch-based composite films is a crucial parameter that can substantially influence their physical properties and functional performance [34]. Table 1 presents water resistance characteristics of neat starch and biocomposite films reinforced with VT and TVT. The MS content of SS_VT was lower than that of SS and SS_TVT films. This may be due to untreated VT contain noncellulosic components such as waxes, lignin and other organic substances which are less hydrophilic, resulting in a lower water content in the SS_VT film structure than the SS_TVT. Another aspect is that after treatment, more hydroxyl groups appear, leading to increased MS absorption through hydrogen bonding [34–36].

WA can compromise the barrier properties of starch-based films, especially when used in packaging applications. The WA of biocomposite film is the amount of water which can be absorbed

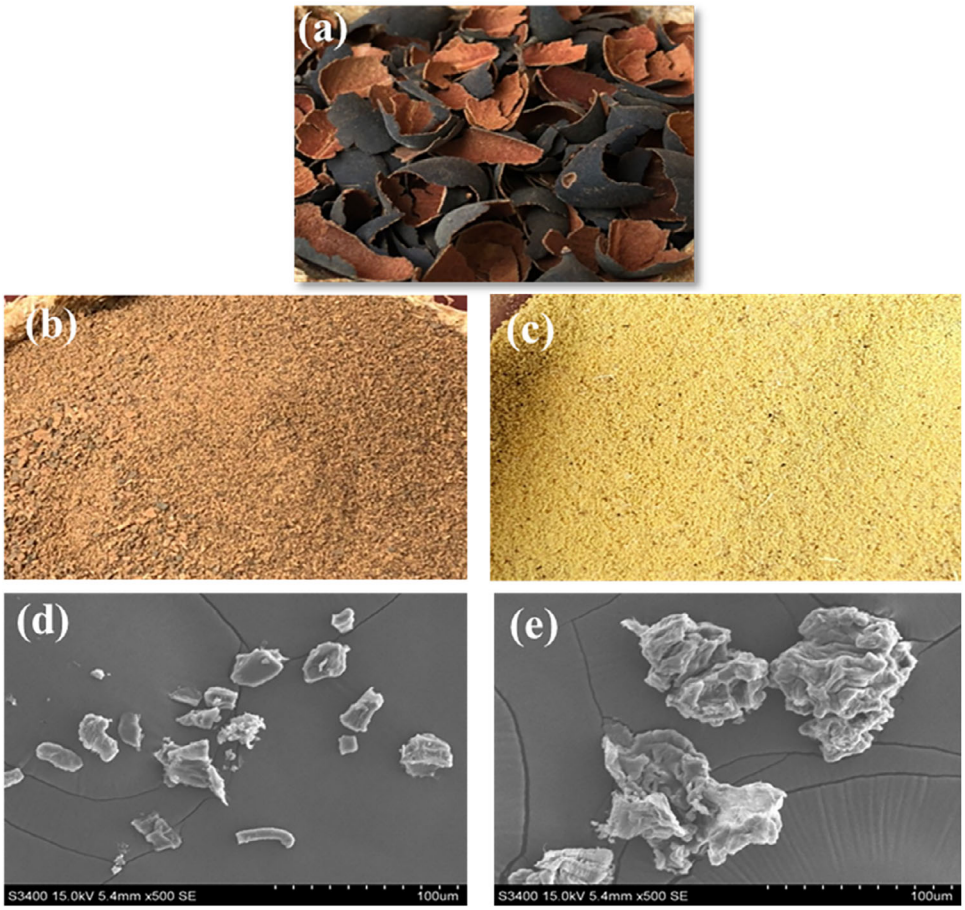

FIGURE 1 | Photographs of velvet tamarind peel (a), VT (b), and TVT (c): SEM images of VT (d) and TVT (e).

TABLE 1 | Water resistance properties of starch and biocomposite films reinforced with VT and TVT.

Biocomposite films	MS (%)	WA (%)	WS at 3 months (%)	WVT (g/cm^2.h)
SS	15.57 ± 0.26	95.43 ± 5.14	34.04 ± 0.22	0.00134 ± 8.72x10^{-5}
SS_VT1	13.41 ± 0.21	80.17 ± 1.34	33.52 ± 0.36	0.00102 ± 7.53x10^{-5}
SS_VT3	14.59 ± 0.33	77.9 ± 2.03	30.45 ± 1.68	0.00106 ± 6.71x10^{-5}
SS_VT5	14.46 ± 0.22	83.6 ± 3.88	29.32 ± 0.61	0.00073 ± 5.90x10^{-5}
SS_TVT1	17.10 ± 0.77	76.97 ± 3.32	30.47 ± 0.32	0.00092 ± 7.18x10^{-5}
SS_TVT3	17.97 ± 0.09	71.54 ± 1.96	29.74 ± 1.22	0.00102 ± 4.57x10^{-5}
SS_TVT5	17.42 ± 0.46	76.01 ± 1.95	45.14 ± 4.70	0.00105 ± 1.25x10^{-4}

under specific conditions. The presence of cellulose fibers in biocomposites decreased the amount of WA [35]. As considered in Table 1, the biocomposites with TVT showed the reduction of WA comparing with SS_VT biocomposites. This is owing to fiber treatment typically removes noncellulosic components such as hemicellulose, lignin, pectin, waxes, and other extractives from VT fibers. The elimination of these amorphous constituents reduces capability of free hydroxy groups to interact with water molecules. In addition, SS_TVT biocomposite films, which have more cellulose content giving more crystalline, showed a lower water binding capacity. Moreover, the incorporation of cellulose fibers significantly reduced the WA of thermoplastic starch (TPS), which can be attributed to more interfacial interaction between cellulose fibers on the starch matrix [38, 39].

The WS is a crucial property of starch-based biocomposite films. For certain applications, water insolubility may be necessary to improve product integrity and extend shelf life [38]. The WS of the neat starch film was about 34%, while the WS of biocomposite films with VT slightly decreased with amount of VT. In the case of TVT, it was found that the WS of biocomposites with 1% and 3% by weight of TVT declined. The reduced solubility suggested that intermolecular interactions occurred between starch and VT in the starch-based composites. The hydroxyl groups on the glucose

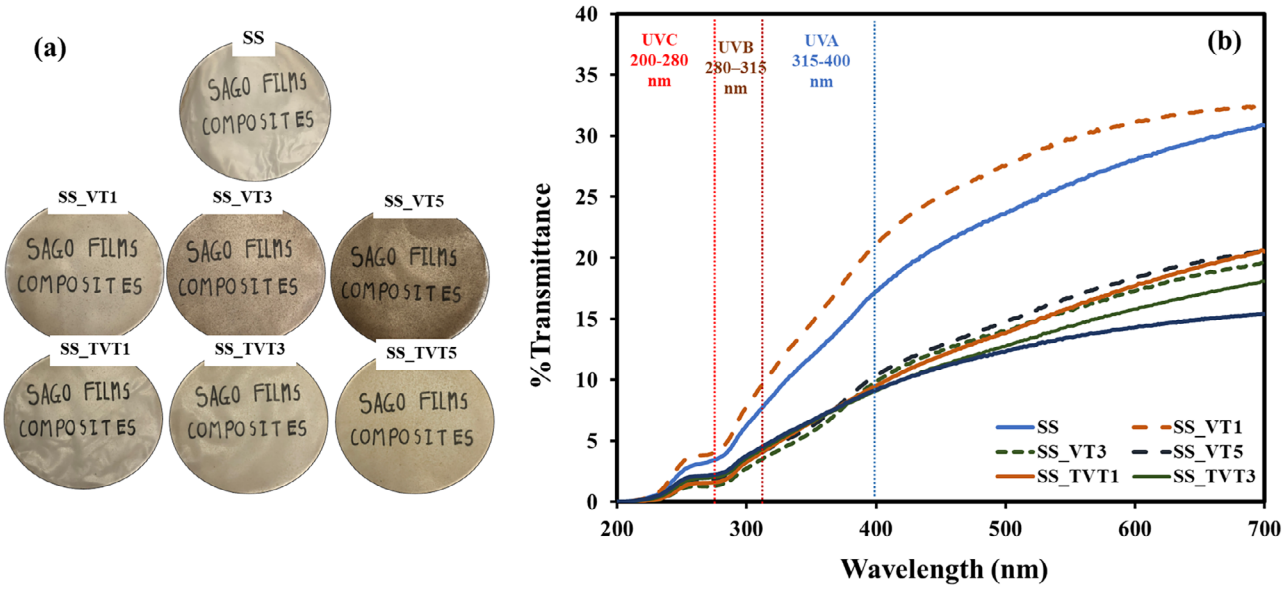

FIGURE 2 | (a) Visual appearances and (b) % transmittance of SS and biocomposite films reinforced with VT and TVT.

units in the cellulose chains can form strong hydrogen bonds with hydroxyl groups on starch, enhancing molecular interactions, improving the cohesiveness of the biopolymer matrix, and reducing WS [40]. When the fiber content reached 5 wt%, an increase in WA was observed. This is due to agglomerate of fiber, resulting in poor dispersion in the starch.

WVT indicates the ability of a film to allow water vapor to pass through, making it a critical property for food packaging applications [37]. The SS film exhibited higher WVT compared to starch films reinforced with VT and TVT. This reduction in WVT can be attributed to the interaction between cellulose and starch, which promotes the formation of hydrogen bonds and increases the compactness of the network structure. As a result, the mobility of polymer chains within the starch matrix was restricted, creating a more tortuous pathway for water molecules and thereby limiting their diffusion. Additionally, cellulose possesses a high-water retention capacity, allowing it to trap a substantial amount of water molecules within the starch matrix [41]. When VT was incorporated up to 5 wt%, WVT significantly decreased, due to the presence of hydrophobic lignocellulosic components, which act as an effective water vapor barrier. Water molecules encounter difficulty penetrating the crystalline regions of cellulose within the film, a phenomenon attributed to increased tortuosity and the reduced availability of hydrophilic sites, thereby limiting water diffusion through the biocomposite films [4, 42]. In contrast, the WVT of SS_TVT composites slightly increased with rising TVT content, which can be explained by the formation of structural irregularities and voids between cellulose particles and the starch matrix. These microscopic gaps provide additional pathways for water vapor, resulting in a modest increase in WVT [41].

ANOVA results of all dependent variables for water resistance characteristics are shown in Table 2. For MS content, the ANOVA results indicate that both FT and FP have significant effects, with p values less than 0.01 and 0.05, respectively. However, the interaction between FT does not significantly affect MS content, as indicated by a p value of 0.494, which is greater than 0.05.

TABLE 2 | ANOVA results (p value) of all dependent variables for water resistance properties.

Variable	MS content	WA content	WVT
FT	< 0.001**	< 0.001**	0.193
FP	0.016*	0.013*	0.035*
FT:FP	0.494	0.344	0.002**
CV%	11.6	5.64	14.3
Adjusted *R*-squared	0.918	0.655	0.611

*Significant at 95% confidence level.
**Significant at 99% confidence level.

A similar trend was observed for WA content, where FT and FP exhibit significant effects with p values below 0.01 and 0.05, respectively, while the interaction term (FT) shows no significant influence ($p = 0.344$). For WVT, FP significantly affects WVT ($p < 0.05$), and the FT is also significant at the 99% confidence level ($p < 0.01$), indicating a meaningful interplay between these factors. However, FT alone does not significantly affect WVT, with a p value of 0.193, suggesting that the effects of FP and FT are independent of FT in this research.

3.4 | Tensile Properties

The stress–strain relationship graph of TPS and starch composite materials containing VT and TVT in amounts of 1, 3, and 5 wt% is shown in Figure 3. The tensile properties of SS_VT composite films are more prone to fracture than that of SS_TVT composites.

Figure 4 illustrates the TS, Young's modulus (YM), and EB of SS_VT, and SS_TVT biocomposite films. The results indicate that both TS and YM of SS composites increased noticeably with VT and TVT content up to 3 wt%. The TS and YM of the

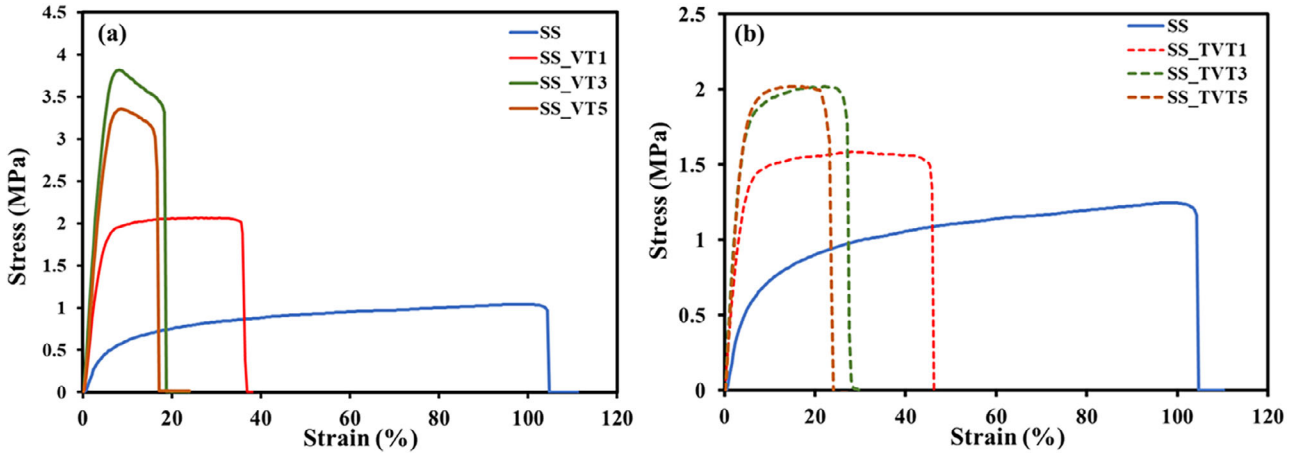

FIGURE 3 | Stress–strain curves for SS and biocomposites reinforced with 1, 3, and 5 wt% of VT (a) and TVT (b).

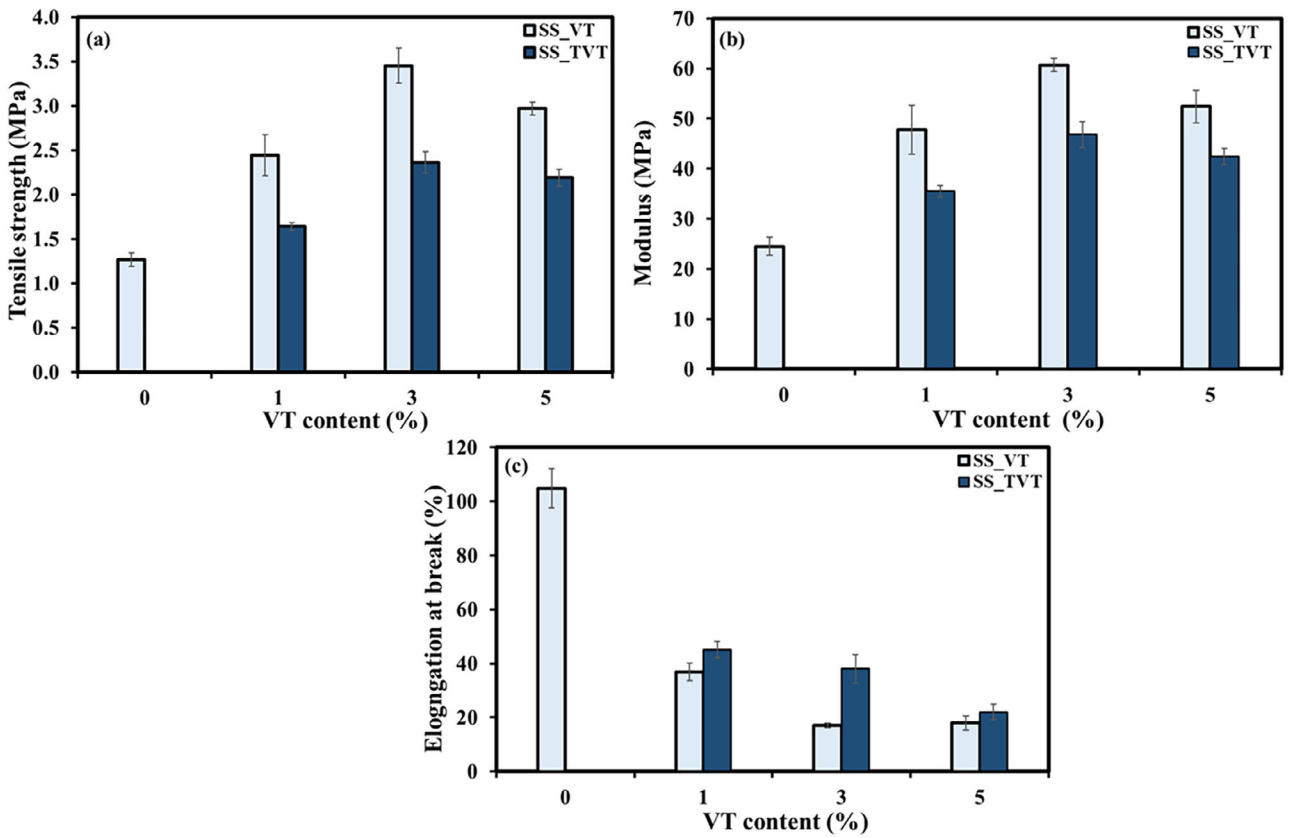

FIGURE 4 | Tensile strength (a), modulus (b), and elongation at break (c).

biocomposites improved as VT was incorporated into the starch matrix, reaching a maximum at 3 wt% VT. The enhancement is attributed to strong interfacial interactions between starch and VT particles, which facilitate effective stress transfer [36]. This is also due to interaction between starch and the lignin or hemicellulose insisting on untreated VT [43]. Additionally, the formation of a rigid percolation network of VT particles, resulting from intra- and intermolecular hydrogen bonding among VT and starch matrix, likely contributes to the observed increases in TS and modulus [17, 20, 33]. However, the tensile properties of SS_VT decreased when VT content increased to 5 wt%. This is due to less interaction of both VT and TVT fibers with starch matrix.

It is evident that biocomposite films reinforced with VT exhibited significantly superior mechanical properties than those reinforced with TVT, as demonstrated by the remarkable increase in TS and YM. This enhancement was attributed to the small size and good dispersion of VT in the matrix, which promotes strong interfacial interactions between starch and cellulose, primarily via hydrogen bonding [44]. For SS_TVT composite films, it might

TABLE 3 | ANOVA results (p value) of all dependent variables for tensile properties.

	Tensile strength	Elongation at break	Modulus
FT	< 0.001**	< 0.001**	< 0.001**
FP	< 0.001**	< 0.001**	< 0.001**
FT: FP	0.871	0.004**	0.334
CV%	21.6	42.2	17.5
Adjusted R-squared	0.870	0.910	0.900

*Significant at 95% confidence level.
**Significant at 99% confidence level.

be expected that an intermolecular hydrogen bonds of cellulose chain of TVT lead to agglomerate resulting in less dispersion starch matrix [14, 17]. In contrast, the significant decrease in strain at break from approximately 100%–38% for VT and 45% for TVT was primarily due to the entanglement of particles within the matrix, which led to a reduction in the ductility of the biocomposites.

The ANOVA results for TS revealed that both FT and FP significantly affect TS at a significant level of 99% as presented in Table 3.

FT: FP represents the interaction effect between the two independent variables, FT and FP. This interaction effect indicates whether the impact of FT on the dependent variable (TS) depends on the level of FP. In simpler terms, it assesses if the combined influence of FT and FP on the dependent variable is different from what would be expected by considering their individual effects alone. For the TS, the interaction between FT and FP does not have a significant effect on TS at the 95% confidence level, with a p value of 0.871, which exceeds the 0.05 threshold. For EB, both FT and FP, as well as their interaction (FT: FP), demonstrate significant effects at the 99% confidence level. This suggests that both factors and their interplay contribute meaningfully to the variation in EB. In the case of modulus, FT and FP crucially affect the modulus at a 99% significance level. However, similar to the results for TS, the interaction between these two independent variables (FT: FP) does not have a notable impact on the modulus at the 95% confidence level, as the p value of 0.334 exceeds 0.05. This indicates that the effects of FT and FP on modulus are independent on each other. In other words, the influence of FP on the modulus remains unchanged regardless of the type of fiber.

3.5 | FTIR Analysis

The infrared spectra of neat starch and biocomposite films are shown in Figure 5. As considered in Figure 5a, the VT spectrum showed the broad peak at 3309 cm^{-1} relating to the axial deformation of the O—H bond and small peaks around 2914 and 2848 cm^{-1}, corresponding to symmetric and asymmetric CH_2 stretching, which are primarily associated with the presence of cellulose, lignin and other components [31]. Additionally, the peak at 1728 cm^{-1} observed in the VT spectrum was attributed to the C═O stretching vibration mode. This peak can be explained by the formation of carboxylic group due to the presence of organic acid in the VT peel. The small peaks at 1604, 1508, and 1433 cm^{-1}, assigned to aromatic skeletal vibration modes, revealed the characteristic lignocellulosic structure of VT. After treatment of VT, the lignin-related peaks decreased, indicating the removal of lignocellulose [45–48]. The spectra of the biocomposite films exhibited similar features to the neat starch film, with some changes due to interaction with VT and TVT. Notably, the absorption band corresponding to hydroxyl group (—OH) vibration of the polysaccharide chains shifted slightly compared to the SS starch matrix and VT, as observed in the region of 3000–3400 cm^{-1} [41]. This shift may be attributed to the gelatinization process and the alteration of intra- and intermolecular hydrogen-bonding networks between starch molecules in the presence of VT and TVT. In the biocomposite film spectra, the peak at 1641 cm^{-1} corresponded to bound water in the starch film, and the peak at 1409 and 1330 cm^{-1} were associated with —CH_2 scissoring and wagging modes, while the peak at 1149, 1074, and 995 cm^{-1} were assigned to C—O—H and C—O—C stretching vibrations in the anhydroglucose units of the starch, respectively [21]. For SS_VT film spectra, within the wavenumber range of 1030–990 cm^{-1}, two adjacent peaks are distinctly observed at 1014 and 995 cm^{-1}. The appearance of the two peaks in the composites indicated an overlap of signals from starch and VT fiber, with hydrogen bond formation causing changes in the peak positions and sharpness. This phenomenon reflects alterations in the short-range order and the crystalline level of the starch matrix [17, 41]. For SS_TVT film spectra (Figure 5b), broad peak centered at 995 cm^{-1} was detected, which was attributed to the overlapping C—O—C stretching vibration of anhydroglucose units in starch and the cellulose fraction of TVT. The broadening of this peak, further influenced by hydrogen bond formation and changes in crystallinity, provides evidence of the coexistence and molecular interaction between TVT and starch.

3.6 | XRD Analysis

XRD is a technique employed to study the crystallographic structure of materials. Cellulose fiber exhibits characteristic peak in the XRD pattern due to their crystalline structure. The effect of incorporation of VT and TVT on the crystalline structure of biocomposite films was also characterized via XRD as shown in Figure 6.

The broad peaks for VT were observed at 2θ around 17.4° and 22.6° corresponding to the (101) and (002) crystallographic planes, respectively. After treatment and beaching, a higher intensity of peak at 2θ = 22.6° was presented [48, 49]. For SS film, the

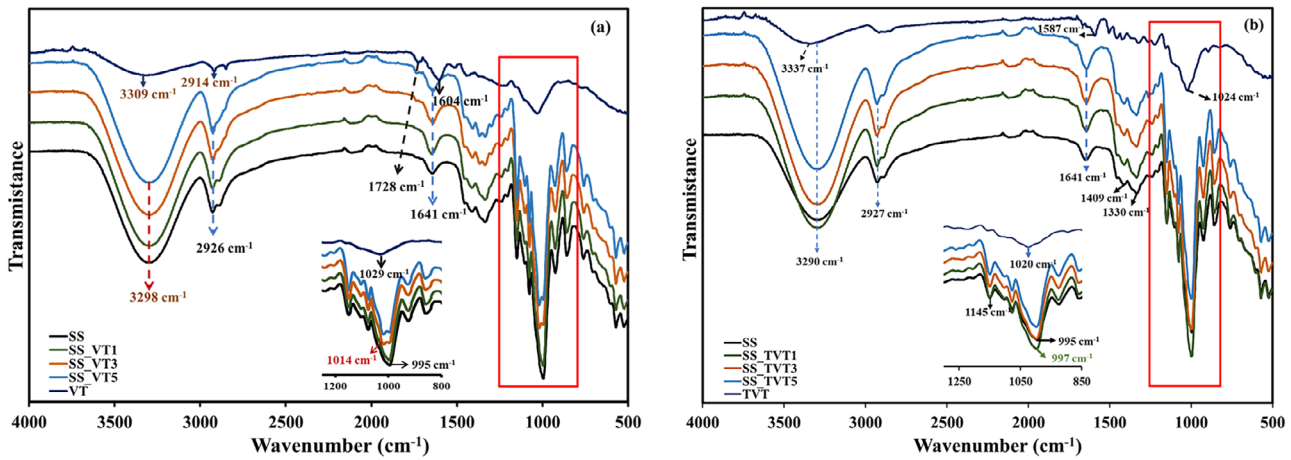

FIGURE 5 | FTIR spectra of biocomposites: (a) SS_VT and (b) SS_TVT.

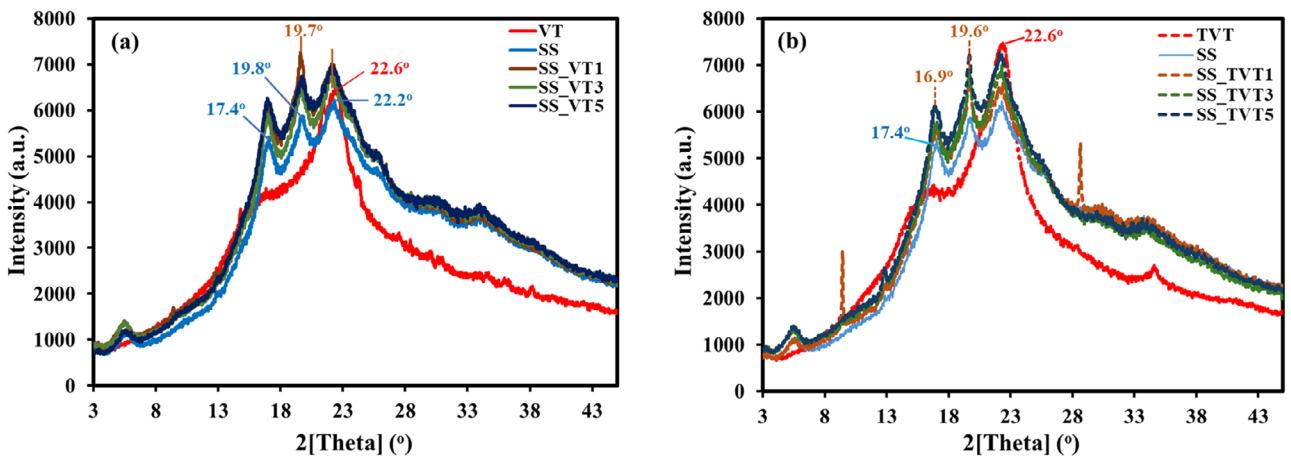

FIGURE 6 | XRD patterns of starch-based composites (a) SS_VT and (b) SS_TVT.

XRD pattern typically showed peak at around $2\theta = 17.4°$ corresponding to the A-type crystalline structure of starch. Notably, the diffraction peaks at $2\theta = 19.8°$ and 22.2° correspond to the (200), and (002) crystallographic planes, respectively, within the starch molecules, indicating alterations in the crystalline structure due to glycerol plasticization [50]. In the XRD pattern of starch-based composites, a combination of peaks from both cellulose and starch indicated the presence of both components in the starch-based composites. In addition, the peak intensity at $2\theta = 17.4°$ of starch composites adding both VT and TVT gradually increased when compared to starch film. This indicates that polysaccharide chain in starch has a more crystallinity and regularly repeat structures within the SS_TVT composites owing to more hydrogen bonding between starch and cellulose [51]. For SS_VT composites, it was assumed that lignocellulose induced the hydrogen bonding between starch and VT particle. This phenomenon leads to the improvement of physical and mechanical properties of biocomposite films.

3.7 | Thermal Stability

TGA and first-derivative thermogravimetric (DTG) curves of the biocomposites are shown in Figure 7. As shown in Figure 7a, glycosidic bonds in VT cellulose were disrupted because of hemicellulose depolymerization in the temperature range of 220°C–300°C. The remarkable weight loss observed between 220°C and 400°C was attributed to the degradation of cellulose, while lignin degradation took place between 450°C and 700°C [52]. The biocomposites were observed to degrade in three stages throughout heating from 40°C to 600°C. The first stage, occurring between 40°C and 150°C, showed a slight weight loss due to MS evaporation [11]. The second stage, with weight loss between 150°C and 260°C, is attributed to the decomposition of glycerol [53]. The third stage, which took place between 280°C and 400°C, is linked to the degradation of starch and cellulose in the biocomposite film. In this stage, the initial thermal decomposition temperature of the composites gradually decreased to lower temperatures as the VT content increased. Thermal degradation temperature of biocomposite films reinforced with 1 wt% of VT and TVT shifted to a temperature higher than that of the starch matrix. It is particularly noteworthy that the incorporation of VT into starch results in a shift of the onset degradation temperature to higher temperatures. Considering the weight loss of samples at a temperature of 150°C, it was found that the biocomposite films added with 1 wt% of VT and TVT had the highest weight loss value. When more VT content was added, the weight loss tended to unchanged, but the onset temperature slightly increased

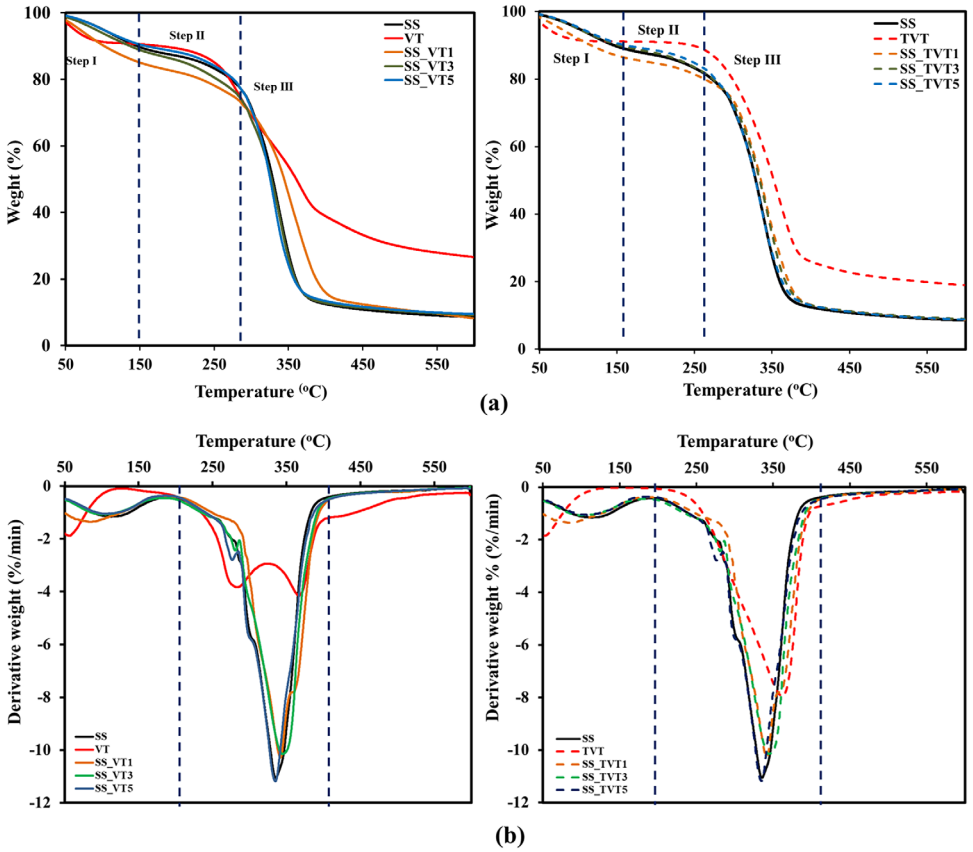

FIGURE 7 | (a) Thermogravimetric (TG) and (b) derivative thermogravimetric (DTG) profiles of SS, VT, TVT, and biocomposite films.

with VT and TVT content. When the temperature increased to 350°C, the weight loss of biocomposite films increased with the increment VT, which is the temperature range where both the starch and the cellulose fiber, decomposition occurred. This can be attributed to the higher thermal stability of the fibers compared to starch, as well as the excellent compatibility between the two polysaccharides. Weight loss behavior is a critical parameter reflecting the thermal stability of starch based composite films. Reduced weight loss, delayed degradation onset, and increased char residue resulting from strong interfacial interactions and enhanced crystalline directly support their future application in thermally demanding, sustainable and biodegradable material systems. Future packaging must withstand heat-sealing processes (>150°C) without significant degradation or weight loss that could compromise structural integrity or release odors.

3.8 | Morphological Study

All specimens revealed microstructure changes and the compatibility between VT or TVT and SS matrix in the cross-sections of the samples as shown in Figure 8. Figure 8a showed the cross-sectional image of the SS film, where a smooth surface was observed with only a few irregularities and no large imperfections. This characteristic can be attributed to the presence of the plasticizer used in film formation. The incorporation of VT (Figure 8b–d) and TVT (Figure 8e–g) in the SS matrix changed their structures with heterogeneity modification of the SS film. The rugosity of the film increased when the increment of VT and TVT content. However, SEM images revealed that the VT particles on the film surface were smaller in size and more uniformly distributed compared to those of TVT. Figure 8d,g presented the biocomposite film morphology with larger imperfections and a rough surface. It was evident that the poor dispersion of VT and TVT in the starch matrix at 5 wt% fiber was due to the aggregation of fillers [54]. More heterogeneous biocomposite films, leading to a brittle film that exhibited a reduced distance at break compared to the starch and the formulations containing 1% and 3% by weight of VT and TVT.

4 | Conclusions

The present study demonstrated the successful development of starch-based composite films reinforced with VT and TVT particles using the solution casting method. The water resistance and tensile properties of SS, SS_VT, and SS_TVT films were investigated. Results revealed that the MS content decreased in SS_VT films but increased in SS_TVT biocomposite films, while both VT and TVT reinforced starch films exhibited lower WA compared to neat SS. Furthermore, the incorporation of VT and TVT enhanced the tensile properties of the biocomposite films, although TVT-reinforced films displayed inferior performance relative to VT due to greater particle agglomeration, as confirmed by SEM observation. Among the formulations, the SS_VT film with 3 wt% of VT exhibited superior mechanical and physical properties. These findings suggest that VT serves as a

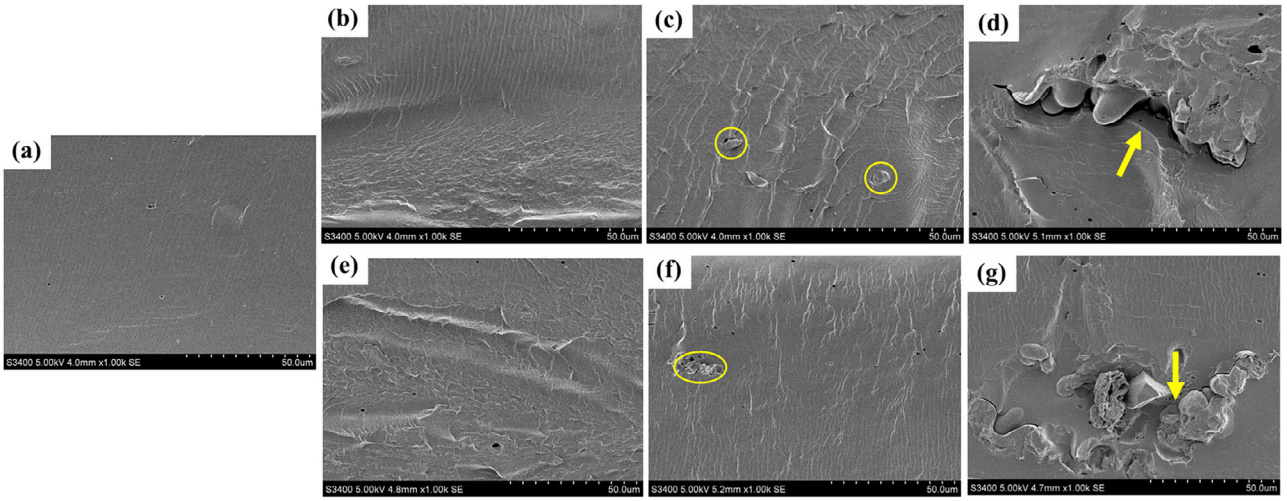

FIGURE 8 | SEM images of cross-sectional view of the control film, biocomposite films; (a) SS, (b) SS_VT1, (c) SS_VT3, (d) SS_VT5, (e) SS_TVT1, (f) SS_TVT3, and (g) SS_TVT5.

promising filler for starch-based films, offering potential as an environmentally friendly and sustainable packaging material.

Author Contributions

Polphat Ruamcharoen: methodology, formal analysis, investigation, data curation, and writing – original draft. **Purintorn Chanlert**: data curation and writing – review and editing. **Chumphon Numuang**: methodology, investigation, and writing – review and editing. **Lapporn Vayachuta**: formal analysis, investigation, and writing – review and editing. **Jareerat Ruamcharoen**: conceptualization, methodology, writing – original draft, review and editing, and project administration.

Conflicts of Interest

The authors declare no conflicts of interest.

Data Availability Statement

The data that support the findings of this study are available from the corresponding author upon reasonable request.

References

1. D. D'Amato and J. Korhonen, "Integrating the Green Economy, Circular Economy and Bioeconomy in a Strategic Sustainability Framework," *Ecological Economics* 188 (2021): 107143.

2. M. R. M. Asyraf, T. Khan, A. Syamsir, and A. B. M. Supian, "Synthetic and Natural Fiber-Reinforced Polymer Matrix Composites for Advanced Applications," *Materials* 15 (2022): 14–16, https://doi.org/10.3390/ma15176030.

3. Z. Boz, V. Korhonen, and C. K. S, "Consumer Considerations for the Implementation of Sustainable Packaging: A Review," *Sustainability* 12 (2020): 1–34.

4. S. P. Bangar and W. S. Whiteside, "Nano-Cellulose Reinforced Starch Bio Composite Films—A Review on Green Composites," *International Journal of Biological Macromolecules* 185 (2021): 849–860, https://doi.org/10.1016/j.ijbiomac.2021.07.017.

5. A. Das, T. Ringu, S. Ghosh, and N. Pramanik, "A Comprehensive Review on Recent Advances in Preparation, Physicochemical Characterization, and Bioengineering Applications of Biopolymers," *Polymer Bulletin* 80 (2023): 7247–7312, https://doi.org/10.1007/s00289-022-04443-4.

6. R. K. Gupta, P. Guha, and P. P. Srivastav, "Natural Polymers in Bio-Degradable/Edible Film: A Review on Environmental Concerns, Cold Plasma Technology and Nanotechnology Application on Food Packaging—A Recent Trends," *Food Chemistry Advances* 1 (2022): 100135, https://doi.org/10.1016/j.focha.2022.100135.

7. V. Prasad, A. Alliyankal Vijayakumar, T. Jose, and S. C. George, "A Comprehensive Review of Sustainability in Natural-Fiber-Reinforced Polymers," *Sustainability* 16 (2024): 1223, https://doi.org/10.3390/su16031223.

8. J. S. Reinaldo, C. H. R. Milfont, F. P. C. Gomes, et al., "Influence of Grape and Acerola Residues on the Antioxidant, Physicochemical and Mechanical Properties of Cassava Starch Biocomposites," *Polymer Testing* 93 (2021): 107015, https://doi.org/10.1016/j.polymertesting.2020.107015.

9. C. Shanbhag, R. Shenoy, P. Shetty, M. Srinivasulu, and R. Nayak, "Formulation and Characterization of Starch-Based Novel Biodegradable Edible Films for Food Packaging," *Journal of Food Science and Technology* 60 (2023): 2858–2867, https://doi.org/10.1007/s13197-023-05803-2.

10. C. L. Luchese, J. M. F. Pavoni, N. Z. dos Santos, et al., "Effect of Chitosan Addition on the Properties of Films Prepared With Corn and Cassava Starches," *Journal of Food Science and Technology* 55 (2018): 2963–2973, https://doi.org/10.1007/s13197-018-3214-y.

11. J. S. Santana, K. de Carvalho Costa, P. R. Rodrigues, P. R. C. Correia, R. S. Cruz, and J. I. Druzian, "Morphological, Barrier, and Mechanical Properties of Cassava Starch Films Reinforced With Cellulose and Starch Nanoparticles," *Journal of Applied Polymer Science* 136 (2019): 1–10, https://doi.org/10.1002/app.47001.

12. J. Ruamcharoen, R. Munlee, L. Vayachuta, and P. Ruamcharoen, "Bio-Based Composites of Sago Starch and Natural Rubber Reinforced With Nanoclays," *Express Polymer Letters* 17 (2023): 1096–1109, https://doi.org/10.3144/expresspolymlett.2023.83.

13. J. Chen, Z. Long, J. Wang, et al., "Preparation and Properties of Microcrystalline Cellulose/Hydroxypropyl Starch Composite Films," *Cellulose* 24 (2017): 4449–4459, https://doi.org/10.1007/s10570-017-1423-6.

14. L. Lendvai, J. Karger-Kocsis, A. Kmetty, and S. X. Drakopoulos, "Production and Characterization of Microfibrillated Cellulose-Reinforced Thermoplastic Starch Composites," *Journal of Applied Polymer Science* 133 (2015): 42397, https://doi.org/10.1002/app.42397.

15. M. M. A. Nassar, K. I. Alzebdeh, T. Pervez, N. Al-Hinai, and A. Munam, "Progress and Challenges in Sustainability, Compatibility, and Production

of Eco-Composites: A State-of-Art Review," *Journal of Applied Polymer Science* 138 (2021): 51284, https://doi.org/10.1002/app.51284.

16. F. Ortega, F. Versino, O. V. López, and M. A. García, "Biobased Composites From Agro-Industrial Wastes and by-Products," *Emergent Materials* 5 (2022): 873–921, https://doi.org/10.1007/s42247-021-00319-x.

17. G. Cheng, M. Zhou, Y. J. Wei, F. Cheng, and P. X. Zhu, "Comparison of Mechanical Reinforcement Effects of Cellulose Nanocrystal, Cellulose Nanofiber, and Microfibrillated Cellulose in Starch Composites," *Polymer Composites* 40 (2019): E365–E372, https://doi.org/10.1002/pc.24685.

18. H. Kargarzadeh, N. Johar, and I. Ahmad, "Starch Biocomposite Film Reinforced by Multiscale Rice Husk Fiber," *Composites Science and Technology* 151 (2017): 147–155, https://doi.org/10.1016/j.compscitech.2017.08.018.

19. S. Collazo-Bigliardi, R. Ortega-Toro, and A. C. Boix, "Reinforcement of Thermoplastic Starch Films With Cellulose Fibres Obtained From Rice and Coffee Husks," *Journal of Renewable Materials* 6 (2018): 599–610, https://doi.org/10.32604/JRM.2018.00127.

20. A. Ali, S. Ali, L. Yu, et al., "Preparation and Characterization of Starch-Based Composite Films Reinforced by Apricot and Walnut Shells," *Journal of Applied Polymer Science* 136 (2019): 47978, https://doi.org/10.1002/app.47978.

21. M. B. Agustin, B. Ahmmad, E. R. P. De Leon, J. L. Buenaobra, J. R. Salazar, and F. Hirose, "Starch-Based Biocomposite Films Reinforced With Cellulose Nanocrystals From Garlic Stalks," *Polymer Composites* 34 (2013): 1325–1332, https://doi.org/10.1002/pc.22546.

22. D. N. A. Wahab, M. B. M. Siddique, J. J. Chew, et al., "Characterization of Starch Biofilm Reinforced With Cellulose Microfibers Isolated From Musa Saba' Midrib Residue and Its Application as an Active Packaging Film," *Journal of Applied Polymer Science* 140 (2023): 1–15, https://doi.org/10.1002/app.54720.

23. Z. Chen, T. Aziz, H. Sun, et al., "Advances and Applications of Cellulose Bio-Composites in Biodegradable Materials," *Journal of Polymers and the Environment* 31 (2023): 2273–2284, https://doi.org/10.1007/s10924-022-02561-8.

24. H. L. Boudjema and H. Bendaikha, "Composite Materials Derived From Biodegradable Starch Polymer and Atriplex Halimus Fibers," *E-Polymers* 15 (2015): 419–426.

25. V. Chanthavong, M. N. Prabhakar, D. W. Lee, and J.-I. Song, "Extraction of Cellulose Microfibers From Waste Fallen Dried Leaves and Fabrication of a Degradable Composite Film for Packaging Applications," *Journal of Inorganic and Organometallic Polymers and Materials* 34 (2023): 1861–1875, https://doi.org/10.1007/s10904-023-02928-x.

26. H. Katong, L. Vayachuta, S. Chotisuwan, and J. Ruamcharoen, "Biocomposites Derived From Esterified Rice Starch Reinforced With Microcellulose Fiber," *Iranian Polymer Journal* 34 (2024): 583–597, https://doi.org/10.1007/s13726-024-01400-y.

27. M. Srisawas, T. Kerdkaew, and P. Chanlert, "From Invasive Species to Bio-Based Composites: Utilizing Water Hyacinth for Sound Absorption and Insulation," *Industrial Crops and Products* 220 (2024): 119242, https://doi.org/10.1016/j.indcrop.2024.119242.

28. M. V. Scatolino, C. S. Fonseca, M. da Silva Gomes, et al., "How the Surface Wettability and Modulus of Elasticity of the Amazonian Paricá Nanofibrils Films Are Affected by the Chemical Changes of the Natural Fibers," *European Journal of Wood and Wood Products* 76 (2018): 1581–1594.

29. M. D. H. Beg, K. L. Pickering, and C. Gauss, "The Effects of Alkaline Digestion, Bleaching and Ultrasonication Treatment of Fibre on 3D Printed Harakeke Fibre Reinforced Polylactic Acid Composites," *Composites Part A: Applied Science and Manufacturing* 166 (2023): 107384, https://doi.org/10.1016/j.compositesa.2022.107384.

30. M. Benali, A. Oulmekki, and J. Toyir, "The Impact of the Alkali-Bleaching Treatment on the Isolation of Natural Cellulosic Fibers From Juncus Effesus L Plant," *Fibers and Polymers* 25 (2024): 525–533, https://doi.org/10.1007/s12221-023-00441-z.

31. S. Ni, H. Bian, Y. Zhang, et al., "Starch-Based Composite Films With Enhanced Hydrophobicity, Thermal Stability, and UV-Shielding Efficacy Induced by Lignin Nanoparticles," *Biomacromolecules* 23 (2022): 829–838, https://doi.org/10.1021/acs.biomac.1c01288.

32. B. C. Maniglia and D. R. Tapia-Blácido, "Structural Modification of Fiber and Starch in Turmeric Residue by Chemical and Mechanical Treatment for Production of Biodegradable Films," *International Journal of Biological Macromolecules* 126 (2019): 507–516, https://doi.org/10.1016/j.ijbiomac.2018.12.206.

33. D. Tian, J. Hu, J. Bao, R. P. Chandra, J. N. Saddler, and C. Lu, "Lignin Valorization: Lignin Nanoparticles as High-Value Bio-Additive for Multifunctional Nanocomposites," *Biotechnology for Biofuels* 10 (2017): 192, https://doi.org/10.1186/s13068-017-0876-z.

34. M. Mahardika, H. Abral, A. Kasim, S. Arief, F. Hafizulhaq, and M. Asrofi, "Properties of Cellulose Nanofiber/Bengkoang Starch Bionanocomposites: Effect of Fiber Loading," *LWT* 116 (2019): 108554, https://doi.org/10.1016/j.lwt.2019.108554.

35. A. I. Quilez-Molina, J. F. Le Meins, B. Charrier, and M. Dumon, "Starch-Fibers Composites, a Study of All-Polysaccharide Foams From Microwave Foaming to Biodegradation," *Carbohydrate Polymers* 328 (2024): 121743, https://doi.org/10.1016/j.carbpol.2023.121743.

36. M. Mohammed, R. Rahman, A. M. Mohammed, et al., "Surface Treatment to Improve Water Repellence and Compatibility of Natural Fiber With Polymer Matrix: Recent Advancement," *Polymer Testing* 115 (2022): 107707, https://doi.org/10.1016/j.polymertesting.2022.107707.

37. J. Long, W. Zhang, M. Zhao, and C. Q. Ruan, "The Reduce of Water Vapor Permeability of Polysaccharide-Based Films in Food Packaging: A Comprehensive Review," *Carbohydrate Polymers* 321 (2023): 121267, https://doi.org/10.1016/j.carbpol.2023.121267.

38. W. Tongdeesoontorn, L. J. Mauer, S. Wongruong, P. Sriburi, and P. Rachtanapun, "Effect of Carboxymethyl Cellulose Concentration on Physical Properties of Biodegradable Cassava Starch-Based Films," *Chemistry Central Journal* 5 (2011): 1–8, https://doi.org/10.1186/1752-153X-5-6.

39. A. Etale, A. J. Onyianta, S. R. Turner, and S. J. Eichhorn, "Cellulose: A Review of Water Interactions, Applications in Composites, and Water Treatment," *Chemical Reviews* 123 (2023): 2016–2048, https://doi.org/10.1021/acs.chemrev.2c00477.

40. B. F. Bergel, L. L. Araujo, and R. M. C. Santana, "Effects of the Addition of Cotton Fibers and Cotton Microfibers on the Structure and Mechanical Properties of Starch Foams Made From Potato Starch," *Carbohydrate Polymer Technologies and Applications* 2 (2021): 100167, https://doi.org/10.1016/j.carpta.2021.100167.

41. J. Zhang, F. Zou, H. Tao, et al., "Effects of Different Sources of Cellulose on Mechanical and Barrier Properties of Thermoplastic Sweet Potato Starch Films," *Industrial Crops and Products* 194 (2023): 116358, https://doi.org/10.1016/j.indcrop.2023.116358.

42. K. Z. Hazrati, S. M. Sapuan, M. Y. M. Zuhri, and R. Jumaidin, "Preparation and Characterization of Starch-Based Biocomposite Films Reinforced by Dioscorea Hispida Fibers," *Journal of Materials Research and Technology* 15 (2021): 1342–1355, https://doi.org/10.1016/j.jmrt.2021.09.003.

43. J. Mohammadi-Rovshandeh, P. Pouresmaeel-Selakjani, S. M. Davachi, B. Kaffashi, A. Hassani, and A. Bahmeyi, "Effect of Lignin Removal on Mechanical, Thermal, and Morphological Properties of Polylactide/Starch/Rice Husk Blend Used in Food Packaging," *Journal of Applied Polymer Science* 131 (2014): 41095, https://doi.org/10.1002/app.41095.

44. X. Cao, Y. Chen, P. R. Chang, A. D. Muir, and G. Falk, "Starch-Based Nanocomposites Reinforced With Flax Cellulose Nanocrystals," *Express Polymer Letters* 2 (2008): 502–510, https://doi.org/10.3144/expresspolymlett.2008.60.

45. A. I. Quilez-Molina, U. C. Paul, D. Merino, and A. Athanassiou, "Composites of Thermoplastic Starch and Lignin-Rich Agricultural Waste for

the Packaging of Fatty Foods," *ACS Sustainable Chemistry & Engineering* 10 (2022): 15402–15413, https://doi.org/10.1021/acssuschemeng.2c04326.

46. P. A. V. Freitas, C. González-Martínez, and A. Chiralt, "Influence of the Cellulose Purification Process on the Properties of Aerogels Obtained From Rice Straw," *Carbohydrate Polymers* 312 (2023): 120805, https://doi.org/10.1016/j.carbpol.2023.120805.

47. A. I. Quilez-Molina, L. Oliveira-Salmazo, C. Amezúa-Arranz, A. López-Gil, and M. Á. Rodríguez-Pérez, "Evaluation of the Acid Hydrolysis as Pre-Treatment to Enhance the Integration and Functionality of Starch Composites Filled With Rich-in-Pectin Agri-Food Waste Orange Peel," *Industrial Crops and Products* 205 (2023): 117407, https://doi.org/10.1016/j.indcrop.2023.117407.

48. L. H. Zaini, A. Solt-Rindler, C. Hansmann, S. Veigel, and W. Gindl-Altmutter, "Lightweight Cellulosic Insulation Panels Made From Oil Palm Trunk Fibers," *Industrial Crops and Products* 222 (2024): 119497, https://doi.org/10.1016/j.indcrop.2024.119497.

49. F. M. Pelissari, P. J. D. A. Sobral, and F. C. Menegalli, "Isolation and Characterization of Cellulose Nanofibers From Banana Peels," *Cellulose* 21 (2014): 417–432, https://doi.org/10.1007/s10570-013-0138-6.

50. K. Dome, E. Podgorbunskikh, A. Bychkov, and O. Lomovsky, "Changes in the Crystallinity Degree of Starch Having Different Types of Crystal Structure After Mechanical Pretreatment," *Polymers* 12 (2020): 641, https://doi.org/10.3390/polym12030641.

51. K. M. Tavares, A. de Campos, B. R. Luchesi, A. A. Resende, J. E. de Oliveira, and J. M. Marconcini, "Effect of Carboxymethyl Cellulose Concentration on Mechanical and Water Vapor Barrier Properties of Corn Starch Films," *Carbohydrate Polymers* 246 (2020): 116521, https://doi.org/10.1016/j.carbpol.2020.116521.

52. J. Wang, E. Minami, M. Asmadi, and H. Kawamoto, "Effect of Delignification on Thermal Degradation Reactivities of Hemicellulose and Cellulose in Wood Cell Walls," *Journal of Wood Science* 67 (2021): 19, https://doi.org/10.1186/s10086-021-01952-0.

53. N. Nordin, S. H. Othman, S. A. Rashid, and R. K. Basha, "Effects of Glycerol and Thymol on Physical, Mechanical, and Thermal Properties of Corn Starch Films," *Food Hydrocolloids* 106 (2020): 105884, https://doi.org/10.1016/j.foodhyd.2020.105884.

54. Y. Tian, P. X. Zhu, and M. Zhou, "Microfibrillated Cellulose Modified With Urea and Its Reinforcement for Starch-Based Bionanocomposites," *Cellulose* 26 (2019): 5981–5993, https://doi.org/10.1007/s10570-019-02505-x.